

# Study of the Thermodynamic Properties of Thermal Plasmas of Fluoroalkylamine-Air Mixtures

Pafadnam Ibrahim<sup>1</sup>, Kohio Nièssan<sup>1</sup>, Yaguibou Wèpari Charles<sup>1</sup>, Kagoné Abdoul Karim<sup>1</sup>, Koalaga Zacharie<sup>1</sup>, André Pascal<sup>2</sup>

<sup>1</sup>Université Joseph Ki-Zerbo, Laboratoire de Matériaux Environnement, Ouagadougou, Burkina Faso

<sup>2</sup>Université Clermont Auvergne, CNRS, Laboratoire de Physique de Clermont, Clermont-Ferrand, France

Email: pafadnamib@yahoo.fr

**How to cite this paper:** Ibrahim, P., Nièssan, K., Charles, Y.W., Karim, K.A., Zacharie, K. and Pascal, A. (2023) Study of the Thermodynamic Properties of Thermal Plasmas of Fluoroalkylamine-Air Mixtures. *Advances in Materials Physics and Chemistry*, **13**, 85-100.

<https://doi.org/10.4236/ampc.2023.135007>

**Received:** January 25, 2023

**Accepted:** May 28, 2023

**Published:** May 31, 2023

Copyright © 2023 by author(s) and Scientific Research Publishing Inc.

This work is licensed under the Creative Commons Attribution International License (CC BY 4.0).

<http://creativecommons.org/licenses/by/4.0/>



Open Access

## Abstract

Knowledge of thermodynamic properties as well as parameters such as energy density and power flow is important for modeling thermal plasmas of fluoroalkylamine-air mixtures. In this paper, these thermodynamic properties of fluoroalkylamine-air mixture plasmas are calculated in a temperature range of 500 K to 20,000 K at atmospheric pressure and local thermodynamic equilibrium (LTE). The Gibbs free energy minimization method is used to determine the chemical equilibrium compositions of the plasmas that are needed to calculate the thermodynamic properties. These thermodynamic properties are then used to calculate the energy density and power flow of these plasmas. The variation of the energy density is related to the variations of the density and mass enthalpy. We notice that, this energy density increases with the percentage of air in the mixture for temperatures higher than 7000 K. The power flow, which depends also on density, enthalpy mass and sound speed, increases with the percentage of air in the same temperature range. Energy density and power flow results show that increasing air percentage in the mixture can be more interesting for damaging gaseous chemical species such as CF<sub>2</sub>, CO, HCN, and HF appearing at low temperatures with high concentrations.

## Keywords

Fluoroalkylamine, Thermodynamic Properties, Chemical Composition, Energy Density, Power Flow

## 1. Introduction

The environmental and climatic issues related to toxic waste management are

not only ecological but also health issue. The use of thermal plasmas, through specific plasma torches for toxic waste destruction, is so promising [1]. Numerous theoretical and experimental studies have been carried out to understand very well these reactive media [2]-[8]. Indeed, active principles containing fluorinated organic components such as fluoroalkylamines or pyrimidine-based molecules are promising in the agricultural field (pesticides and herbicides) and pharmacology (antibiotics) [9]. The massive use of these molecules will result in a massive increase in waste containing these types of molecules. Developed countries have restrictive waste management policies, which is not the case in developing countries. In these countries, we are assisting in a proliferation of waste open air area storage from some others countries [10]. These practices have a lot of consequences on the environment like air, soil and water pollution. This could affect also human health. One of the solutions which could give better satisfaction about solid waste is use of plasma torches. These torches could reach high temperatures (5000 K to 20,000 K). However, the use of these means of treatment is not without danger because some toxic or lethal molecules could result from it. In order to understand these difficulties, we propose to study the air influence on thermodynamic properties as well as parameters such as energy density and power flow of a plasma based on fluoroalkylamines (trifluoroethylamine:  $C_2H_4F_3N$ , Nonafluoropentylamine:  $C_5H_4F_9N$ , ...), at atmospheric pressure and at local thermodynamic equilibrium (LTE), in a range of temperatures going from 500 K to 20,000 K. More precisely it's calculation of density, enthalpy mass, heat mass at constant pressure and sound speed in the plasma. These parameters are necessary to determine the power flow and the energy density of the plasma. The data obtained can be used for modeling the plasma in the fluoroalkylamine-air mixture. In the framework of our study, we decided to consider only the gaseous phase, to work at atmospheric pressure, to consider that the air is made up of 20% of dioxygen and 80% of nitrogen, and that the various percentages selected are volumetric percentages. As fluoroalkylamines, we will use in this work trifluoroethylamine ( $C_2H_4F_3N$ ) and nonafluoropentylamine ( $C_5H_4F_9N$ ).

Firstly, we will describe the computational methods to get the thermodynamic properties as well as the parameters such as energy density and power flow at atmospheric pressure. Secondly, we will present the results and finally, we will conclude.

## 2. Thermodynamic Properties Calculation Method

Thermodynamic properties as well as energy density and power flow can be deduced from the knowledge of species densities and partition functions, formulations of which are available in the literature [11]-[16].

### 2.1. Chemical Composition of Plasmas

The plasmas studied in this work, are recorded in **Table 1**. The determination of the chemical composition of the plasmas is based on the Gibbs free energy mi-

nimization method using the Newton-Raphson method in the temperature range from 500 K to 20,000 K, at atmospheric pressure and at local thermodynamic equilibrium (LTE). We have considered that air is constituted with 80% of nitrogen ( $N_2$ ) and 20% of oxygen ( $O_2$ ), the other components (Ar,  $CO_2$ ,  $CH_4$ , ...) have been totally neglected. The chemical species considered in the fluoroalkylamine-air mixture plasma are:

- electrons:  $e^-$ ;
- monoatomic species (18): C,  $C^+$ ,  $C^{2+}$ ,  $C^-$ , F,  $F^+$ ,  $F^-$ , H,  $H^+$ ,  $H^-$ , N,  $N^+$ ,  $N^{2+}$ ,  $N^-$ , O,  $O^+$ ,  $O^{2+}$ ,  $O^-$ ;
- diatomic species (27):  $C_2$ ,  $F_2$ ,  $H_2$ ,  $N_2$ ,  $O_2$ , CF, CH, CN, NF, NH, CO, NO, OH, HF,  $C_2^+$ ,  $H_2^+$ ,  $N_2^+$ ,  $O_2^+$ ,  $NO^+$ ,  $CF^+$ ,  $CH^+$ ,  $CN^+$ ,  $NH^+$ ,  $CO^+$ ,  $C_2^-$ ,  $H_2^-$ ,  $CN^-$ ;
- polyatomic species (13):  $CO_2$ ,  $NO_2$ ,  $NO_3$ ,  $CF_2$ ,  $CF_3$ ,  $CH_4$ ,  $C_2F$ ,  $C_2F_2$ ,  $C_2F_3$ ,  $NH_3$ ,  $N_2H_4$ , HCN,  $NO_2^-$ .

## 2.2. Density $\rho$

It measures the sum of mass contained in a cubic meter of plasma and is mentioned in ( $kg \cdot m^{-3}$ ). It is calculated using the mass (kg) and the numerical density ( $m^{-3}$ ) of chemical species in the plasma [11] [13] [14]:

$$\rho = \sum_{j=1}^N n_j m_j \quad (1)$$

where  $n_j$  and  $m_j$  are the number density and mass of species  $j$ , respectively, and  $N$  is the number of species that constitute the plasma.

## 2.3. Mass Enthalpy $h$

The mass enthalpy can be calculated by the following formula [17]:

$$h = \frac{1}{M} \sum_{i=1}^N X_i (h_i^0 + e_i^0) \quad (2)$$

where  $h_i^0$  and  $e_i^0$  are the specific molar enthalpy and the enthalpy of formation of species  $i$ , respectively.

## 2.4. Mass Heat at Constant Pressure $C_p$

It represents the capacity of a system to store heat. If the thermodynamic

**Table 1.** Different plasmas studied.

Mixtures	Notation
100% trifluoroethylamine	trif
100% nonafluoropentylamine.	nonaf
99% trif + 1% air	Mix1
50% trif + 50% air	Mix50
99% nonaf + 1% air	Mix1
50% nonaf + 50% air	Mix50

transformation of the system takes place at constant pressure, the specific heat can be calculated by [13] [14] [18] [19]:

$$C_p = \frac{h_{T+\Delta T} - h_T}{\Delta T} \quad (3)$$

$\Delta T$  is the temperature step.

### 2.5. Sound Velocity in Plasma $a$

The speed of sound or sound velocity is the speed of propagation of waves in a fluid. It is defined as follows [20] [21]:

$$a = \left( \gamma \frac{P}{\rho} \right)^{1/2} \quad (4)$$

where  $\gamma = \frac{C_p}{C_v}$ ,  $\rho$  the density,  $P$  the pressure in the plasma.

### 2.6. Power Flow $\phi$ and Energy Density $De$

The power flow expresses the capacity plasma to evacuate energy to external environment. It is expressed by the following expression [13] [14] [16] [22]:

$$\phi = \rho \cdot h \cdot a \quad (5)$$

The energy density characterizes the distribution of energy in the specific environment. It is defined by the following expression [13] [14] [16]:

$$De = \rho \cdot h \quad (6)$$

## 3. Results and Discussion

In this section, we present results of thermodynamic properties such as densities, enthalpies of mass, heats of mass at constant pressure, sound velocities, and others important parameters for plasma modeling such as energy densities and power flows in trifluoroethylamine and nonafluoropentylamine plasmas. Some results of the plasmas composition are briefly presented. The calculations were performed at atmospheric pressure and LTE.

We first compared our results from calculations density, mass enthalpy and heat capacity at constant pressure of the plasma formed of pure air with those of P. André [7] in **Figures 1-3**. We note that our results are in good agreement with those of P. André. We can note some differences. These differences could be due to the study methods and the data used.

### 3.1. Equilibrium Composition of Plasmas

**Figure 4** and **Figure 5** show the equilibrium compositions of trifluoroethylamine (trif) and nonafluoropentylamine-air (mel'1) plasmas at LTE and atmospheric pressure (1 bar). We notice that, for temperatures beyond 15,000 K, molecular species completely disappear. Numerical densities of atomic species progressively decrease. Those of ions ( $C^+$ ,  $F^+$ ,  $H^+$ ,  $N^+$ ,  $O^+$ ) increase. It is also noticed that ions  $C^{2+}$  and  $N^{2+}$  appear.

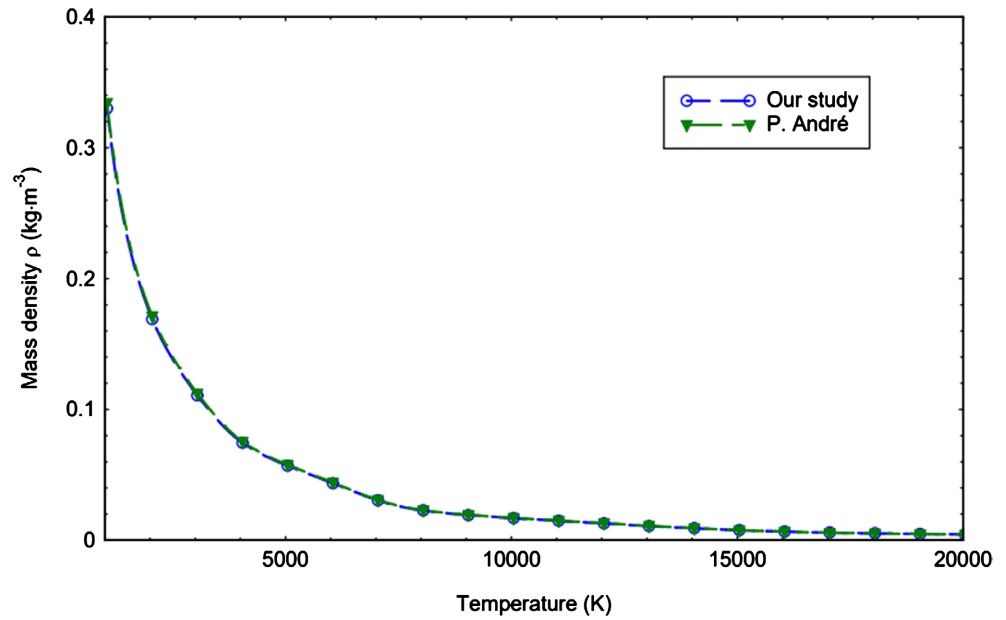


**Figure 1.** Comparison of the density results of our study with those of P. André.

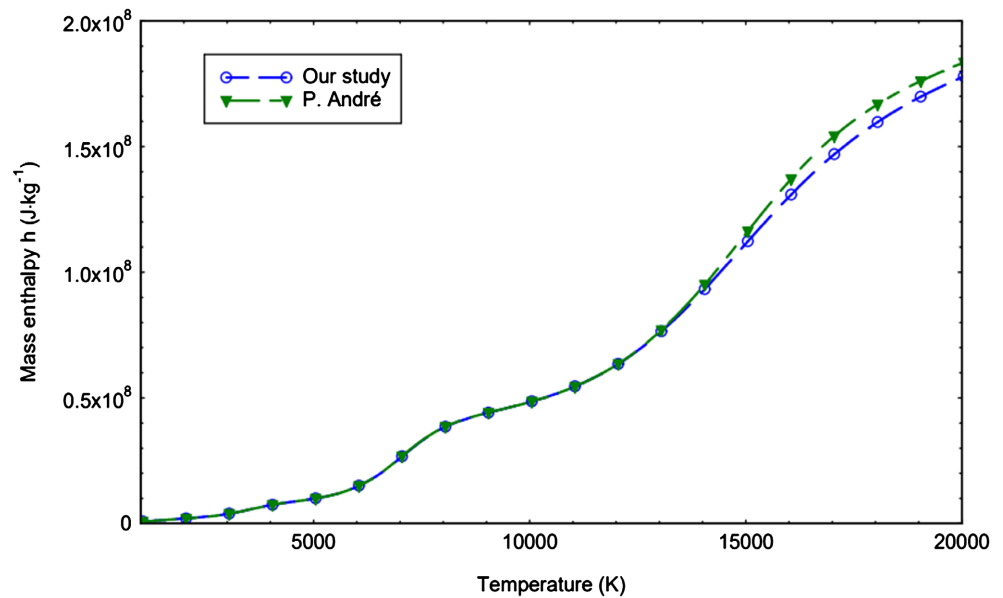


**Figure 2.** Comparison of the results of the mass enthalpies of our study with those of P. André.

### 3.2. Mass Density

We have represented in **Figure 6** and **Figure 7** the evolution according to temperature of trifluoroethylamine (Trif), nonafluoropentylamine (Nonaf), trifluoroethylamine-air (Trif-Air) and nonafluoropentylamine-air (Nonaf-Air) plasmas volumic mass in atmospheric pressure and ETL. Regarding to these different figures, the influence of the air percentage on the density of the trifluoroethylamine plasma is similar to its influence on that of the nonafluoropentylamine plasma. The density decreases with increase of temperature. The decrease following temperature is explained by the rarefaction effect linked to the

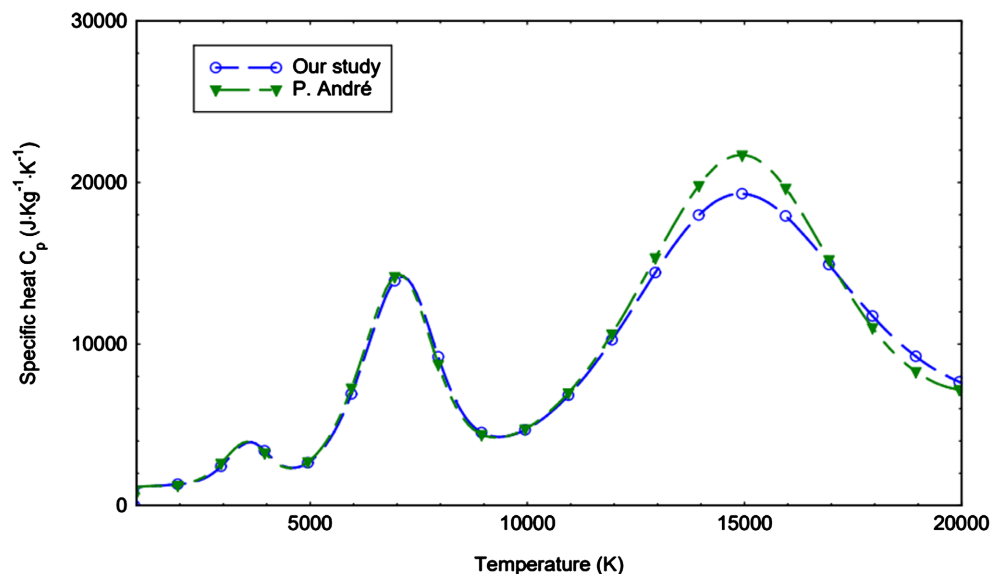


Figure 3. Comparison of the specific heat results of our study with those of P. André.

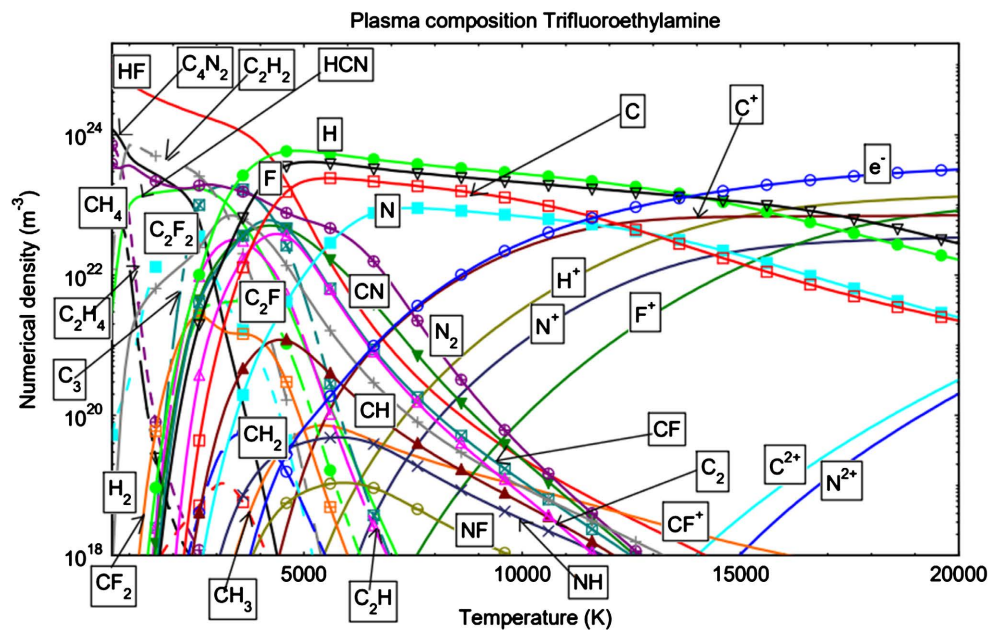
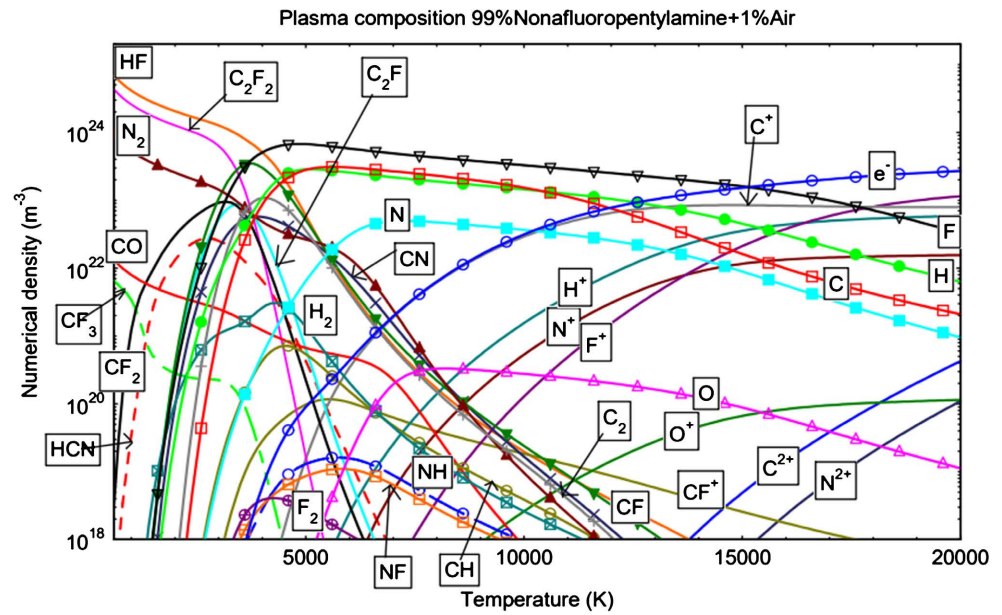


Figure 4. Numerical density variation of trif plasma different particles versus temperature at atmospheric pressure.

law of perfect gases and the dissociation, ionization of molecules progressively replaced at high temperatures by lighter atoms and electrons [23]. In other hand, it increases slightly with the percentage of air for temperatures less than 4500 K. Above this temperature, air has an almost negligible influence on the density. The increase with the percentage of air is not explained only by the increment of species densities in the area but also by chemical reactions that take place.

### 3.3. Mass Enthalpy

Figure 8 and Figure 9 represent the variations of the mass enthalpies of the



**Figure 5.** Numerical density variation of mix'1 plasma different particles versus temperature at atmospheric pressure.

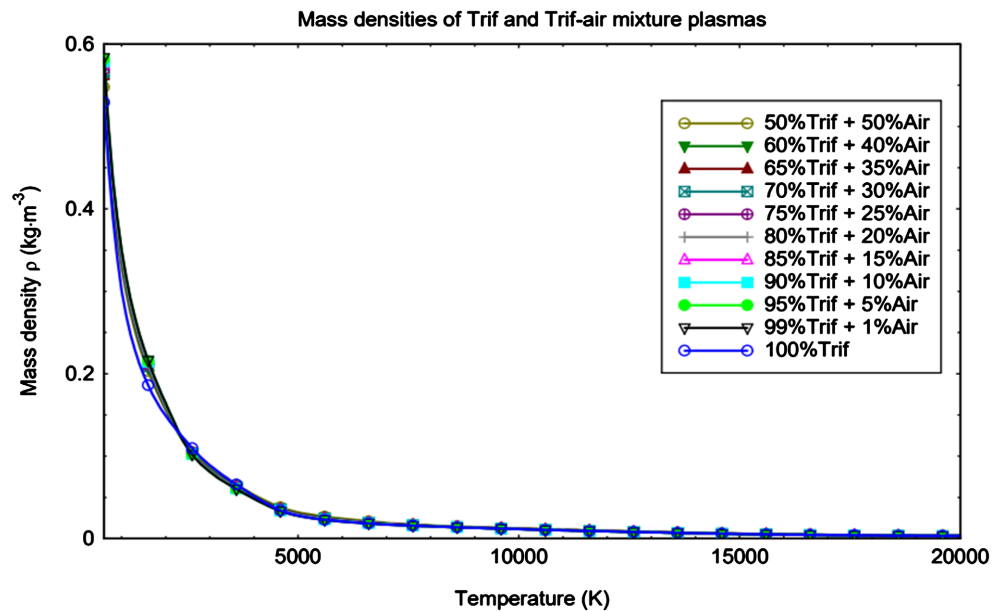


**Figure 6.** Mass density evolution of plasma versus temperature at atmospheric pressure.

trifluoroethylamine-air and nonfluoropentylamine-air mixture plasmas. The curves are plotted as a function of temperature, at LTE and at atmospheric pressure. These curves show similar evolutions. We find a well-known pattern in the literature, which is a continuous and increasing function of the temperature with shows some level of rapid evolution phases corresponding to the reactivity of the area and more particularly to the dissociation and ionization phenomena. This is highlighted by the variations of the heat capacity which depends strongly on the chemical reactions. The mass enthalpy varies lowly with the increase of air



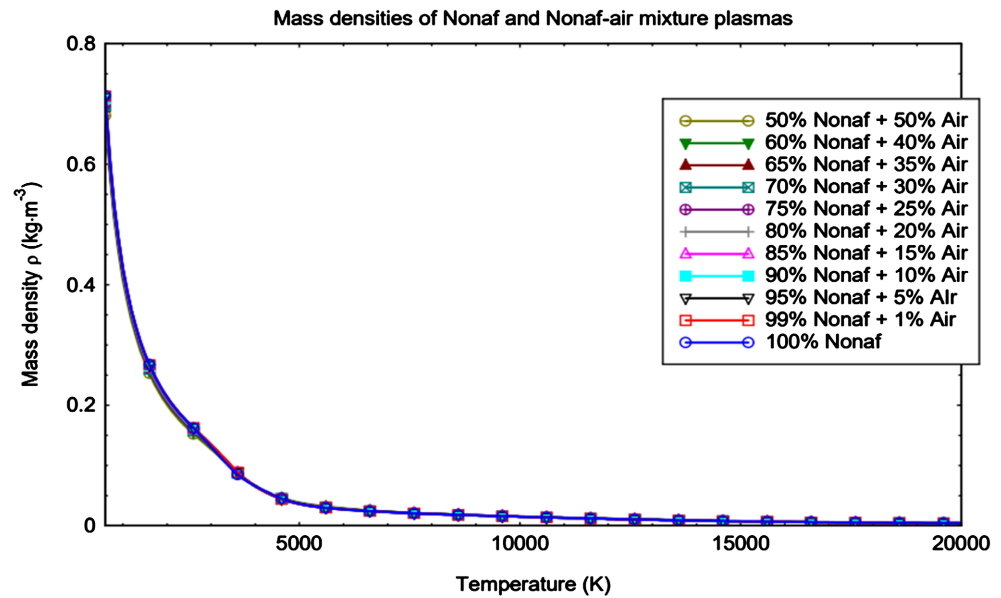


Figure 7. Mass density evolution of plasma versus temperature at atmospheric pressure.

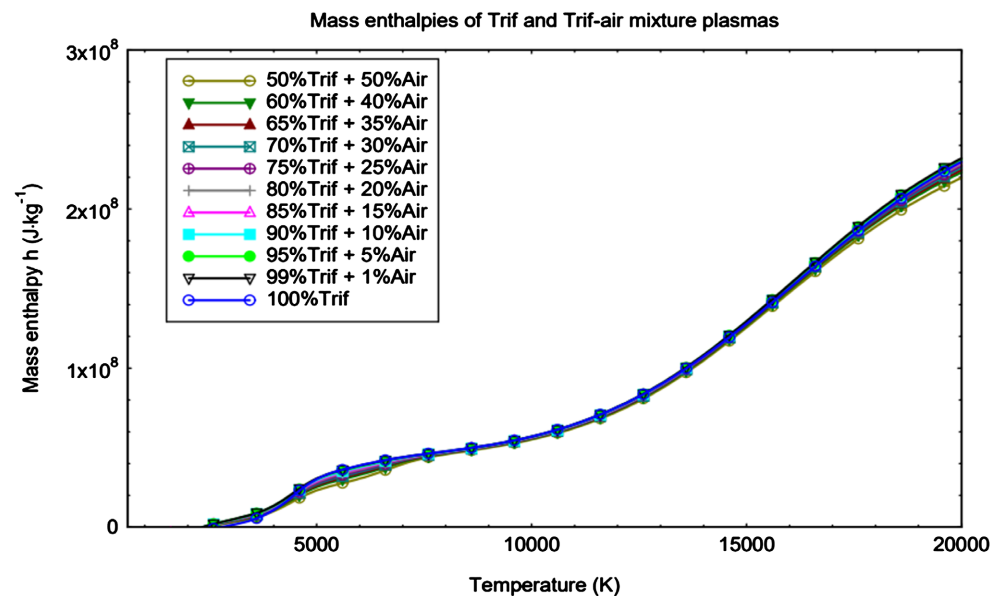


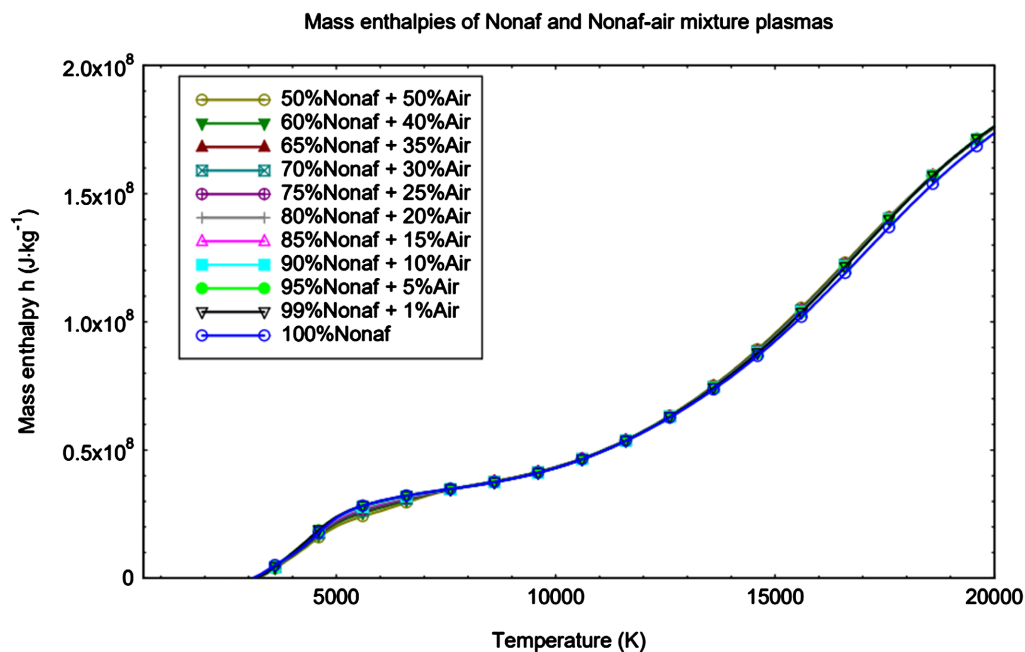
Figure 8. Mass enthalpy evolution of plasma versus temperature at atmospheric pressure.

percentage. However, a slight increase is observed at high temperature ( $T > 14,000$  K).

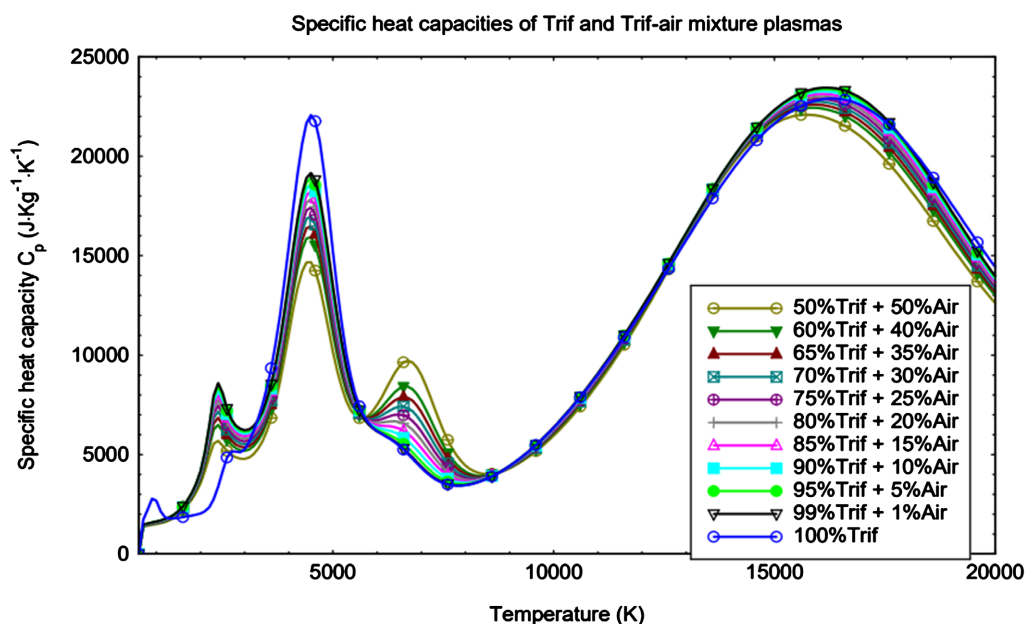
### 3.4. Specific Heat

Figure 10 and Figure 11 show the evolution, according to temperature, the heats of mass at constant pressure of trifluoroethylamine, nonafluoropentylamine, trifluoroethylamine-air and nonafluoropentylamine-air plasmas. These curves show quasi-similar evolutions, with the appearance of peaks. The comparison of these figures with Figure 1 and Figure 2 allows to associate the peaks of the heat capacities to chemical reactions. We observe more peaks in Figure 10





**Figure 9.** Mass enthalpy evolution of plasma versus temperature at atmospheric pressure.



**Figure 10.** Specific heat capacity evolution of plasma versus temperature at atmospheric pressure.

than in **Figure 11**. The peaks appearing around a temperature of 1500 K corresponding to the dissociation of molecules  $\text{C}_2\text{H}_4$  and  $\text{CH}_4$  (**Figure 10**). The peaks appearing around 5000 K result from the dissociation of molecules ( $\text{C}_2\text{H}_2$ ,  $\text{C}_2\text{F}_2$ ) and radicals ( $\text{C}_4\text{N}_2$ ,  $\text{CH}_2$ ,  $\text{CH}_3$ ,  $\text{CF}_3$ ) (**Figure 10** and **Figure 11**). The following peaks located around 7000 K correspond to the dissociation of molecules ( $\text{HCN}$ ,  $\text{F}_2$ ) and radicals ( $\text{C}_2\text{F}$ ,  $\text{CF}_2$ ,  $\text{C}_3$ ,  $\text{C}_2\text{H}$ ). The following peaks located around 15,000 K correspond to the dissociation of molecules ( $\text{HF}$ ,  $\text{C}_2$ ,  $\text{N}_2$ ), radicals ( $\text{CF}$ ,  $\text{CN}$ ,  $\text{CH}$ ,  $\text{CO}$ ) and the ionization of species such as ( $\text{F}$ ,  $\text{H}$ ,  $\text{N}$ ,  $\text{C}$ ,  $\text{O}$ ,  $\text{N}^+$ ).

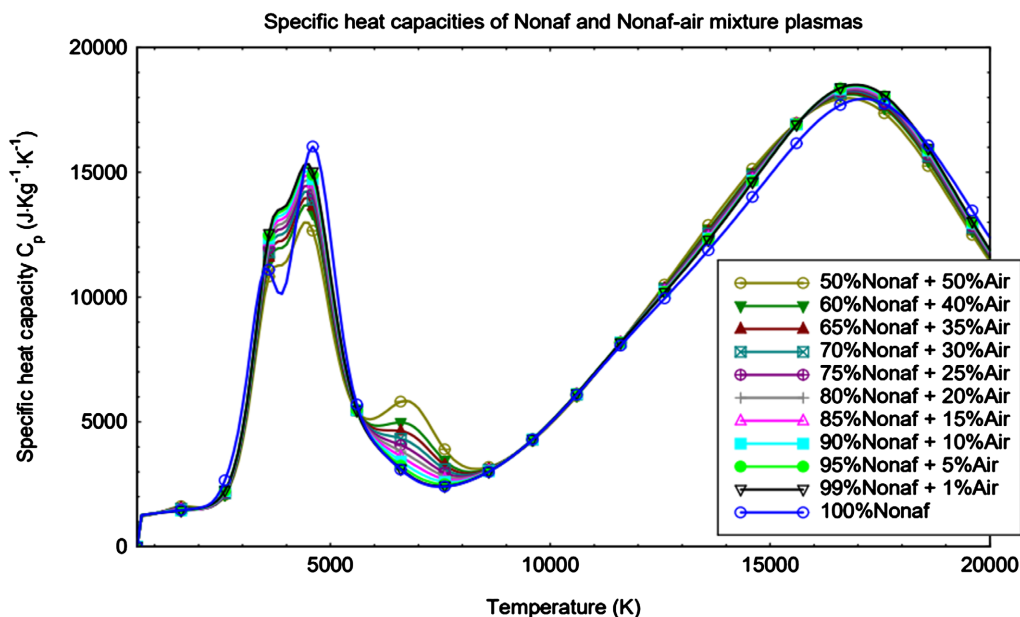


Figure 11. Specific heat capacity evolution of plasma versus temperature at atmospheric pressure.

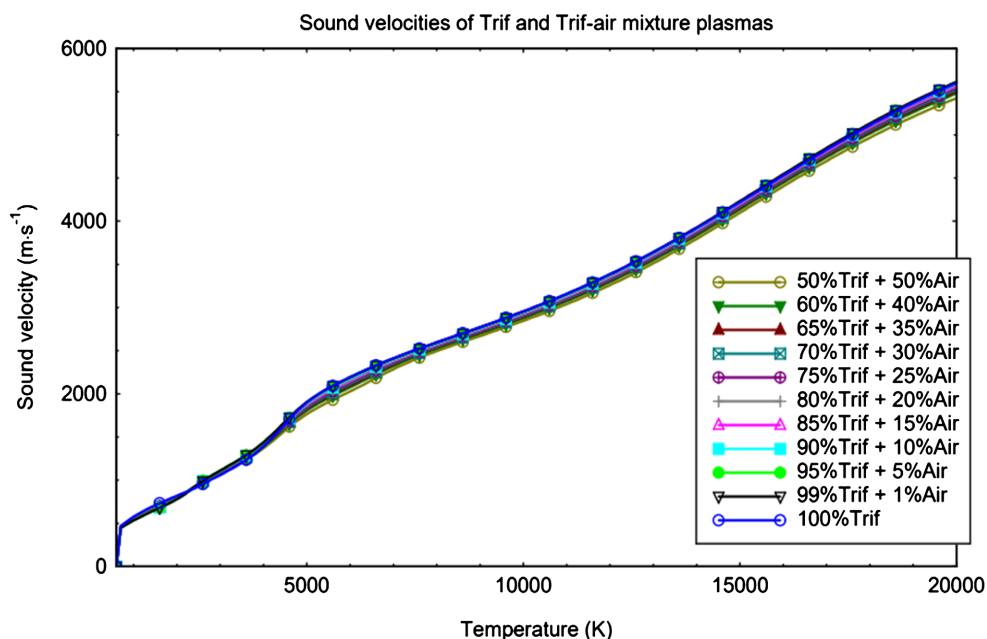


Figure 12. Sound velocity variation in plasma versus temperature at atmospheric pressure.

### 3.5. Sound Velocity

Figure 12 and Figure 13 represent the variation according to temperature, air percentage, the sound velocities in plasmas, trifluoroethylamine, nonafluoropentylamine, trifluoroethylamine-air and nonafluoropentylamine-air mixture. The sound speed in the plasma increases with temperature. In general, the sound velocity decreases slightly with the percentage of air for the Trifluoroethylamine-air mixture plasma. On other hand, the percentage of air has a negligible influence on the Nonafluoropentylamine-air mixture plasma.

### 3.6. Energy Density

Figure 14 and Figure 15 show air influence on energy densities of trifluoroethylamine, nonafluoropentylamine, trifluoroethylamine-air and nonafluoropentylamine-air plasmas. Between 500 K and 7000 K, the energy densities of trifluoroethylamine and nonafluoropentylamine plasmas decrease with the percentage of air in the mixture. They increase with the percentage of air for both plasmas between 7000 K and 20,000 K.

### 3.7. Power Flow

To better appreciate the influence of air on plasmas power flows, we varied the

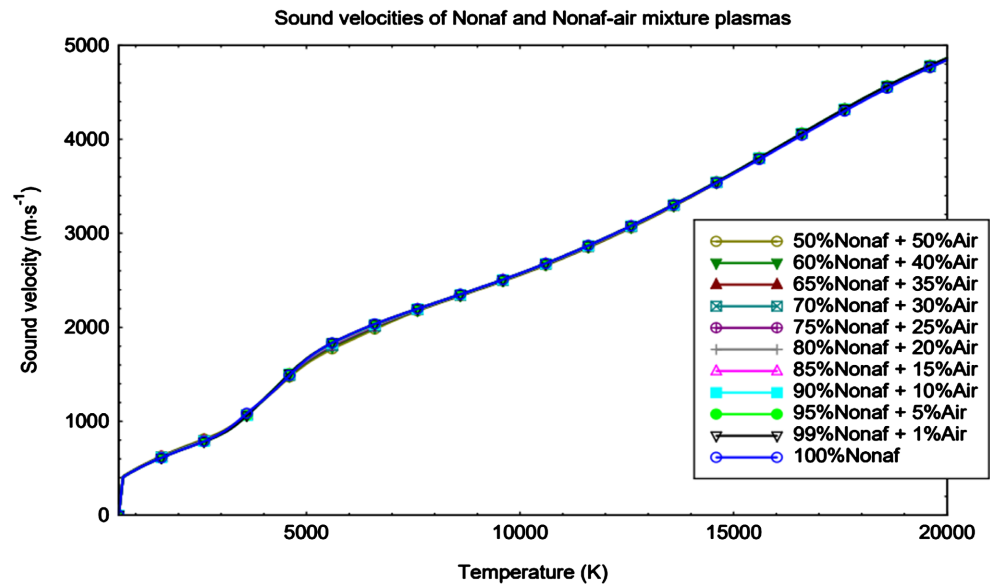


Figure 13. Sound velocity variation in plasma versus temperature at atmospheric pressure.

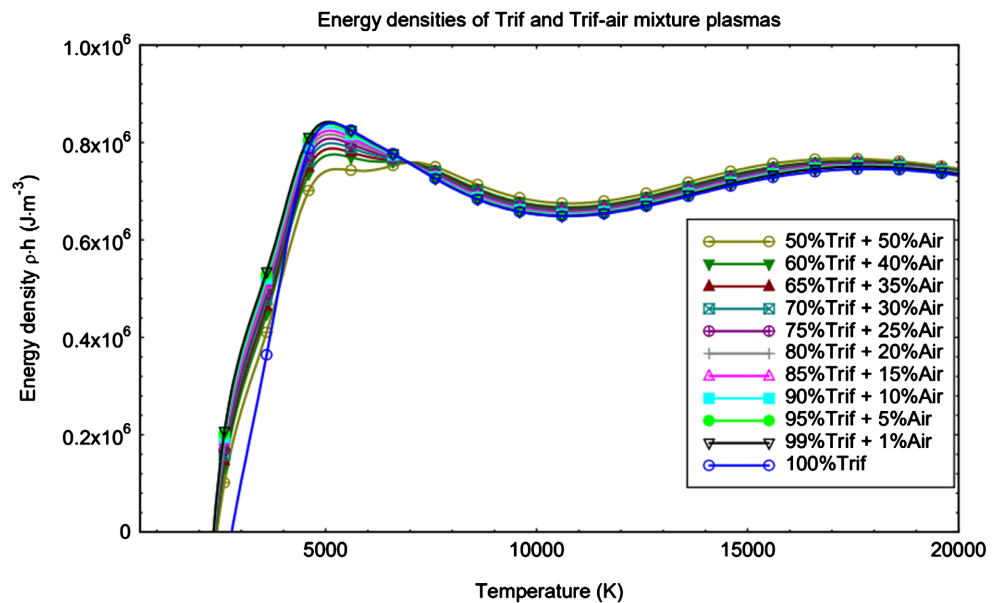
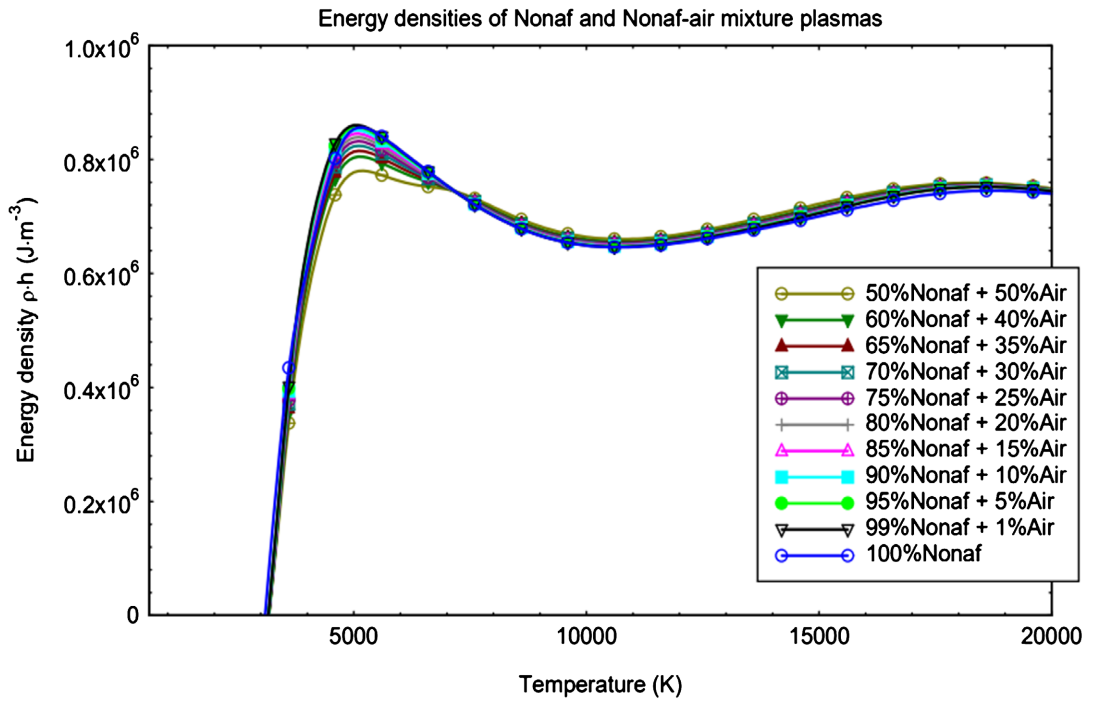
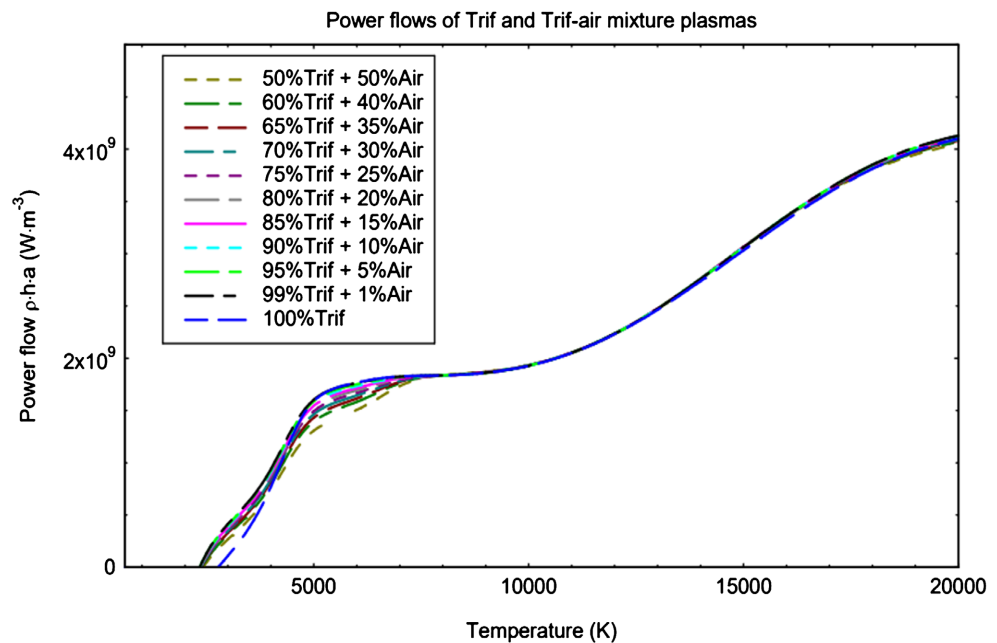


Figure 14. Energy density variation of plasma versus temperature at atmospheric pressure.

air content in the mixtures from 1% to 50%. **Figure 16** and **Figure 17** show the evolution of the power flows of the plasmas studied at atmospheric pressure and at LTE as a function of temperature. These power flows are important characteristics for the modelization of plasmas. Between 500 K and 7000 K, the power flow for trifluoroethylamine and nonafluoropentylamine plasmas decreases with the percentage of air in the mixture. The flow stay invariant with the percentage



**Figure 15.** Energy density variation of plasma versus temperature at atmospheric pressure.



**Figure 16.** Power flow variation of plasma versus temperature at atmospheric pressure.

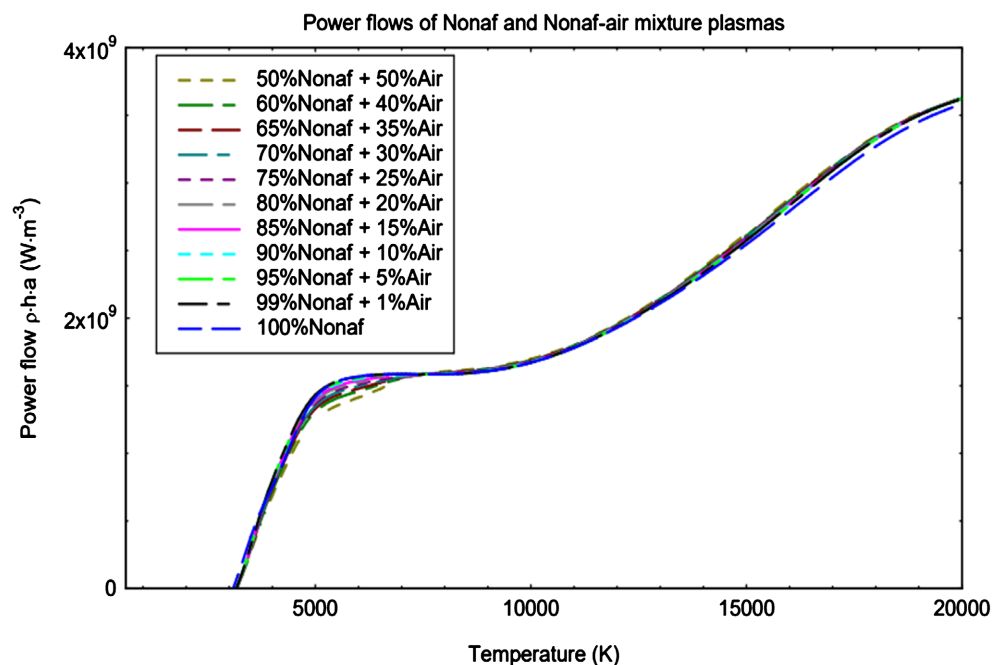


**Figure 17.** Power flow variation of plasma versus temperature at atmospheric pressure.

of trifluoroethylamine plasma air between 7000 K and 20,000 K. In other hand, it slightly increases with the percentage of air for the nonafluoropentylamine plasma in the same temperature range.

#### 4. Conclusion

In this paper, we have presented and analyzed the results of thermodynamic properties as well as parameters such as energy densities and power flows that are important for modeling thermal plasmas of trifluoroethylamine, nonafluoropentylamine, trifluoroethylamine-air and nonafluoropentylamine-air mixtures at local thermodynamic equilibrium and at atmospheric pressure. From the analysis, it appears that:

- the density decreases with increasing temperature. In other hand, it increases slightly with the percentage of air for temperatures lower than 4500 K. Above this temperature, the densities are roughly equal;
- the mass enthalpy shows a low variation with the increases of the percentage of air. However, a slight increase is observed at high temperature ( $T > 14,000$  K);
- when the percentage of air increases, we observe a shift of the peaks of the specific heat of the plasma towards high temperatures and a slight decrease of their values. The comparison of **Figure 10** and **Figure 11**, with **Figure 4** and **Figure 5** allows to associate the peaks of the heat capacities to chemical reactions;
- the sound speed in the plasma increases with temperature. But in general, the air percentage has practically an insignificant influence on the speed of sound in the plasma;

- between 500 K and 7000 K, the energy densities of trifluoroethylamine and nonafluoropentylamine plasmas decrease with the percentage of air in the mixture. They increase with the percentage of air for both plasmas between 7000 K and 20,000 K;
- between 500 K and 7000 K, the power flow for trifluoroethylamine and nonafluoropentylamine plasmas decreases with the percentage of air in the mixture. The flow stays invariant with the percentage of trifluoroethylamine plasma air between 7000 K and 20,000 K. In other hand, it slightly increases with the percentage of air for the nonafluoropentylamine plasma in the same temperature range.

The energy density and power flux results show that increasing percentage of air in the mixture can be even more interesting for the destruction of hazardous and toxic gaseous chemical species such as CF<sub>2</sub>, CO, HCN and HF which appear at low temperatures with high concentration.

We can therefore say that nonafluoropentylamine plasma performs better than trifluoroethylamine plasma.

### Conflicts of Interest

The authors declare no conflicts of interest regarding the publication of this paper.

### References

- [1] Wang, J., Zheng, P. and Cui, H. (2020) Plasma Gasification Melting/Waste Treatment System. *Advances in New and Renewable Energy*, **8**, 391-395. <https://doi.org/10.3969/j.issn.2095-560X.2020.05.007>
- [2] Cressault, Y., Teulet, P., Baumann, X., Vanhulle, G., Reichert, F., Petchanka, A. and Kabbaj, N. (2019) State of Art and Challenges for the Calculation of Radiative and Transport Properties of Thermal Plasmas in HVCB. *Plasma Physics and Technology*, **6**, 208-216. <https://doi.org/10.14311/ppt.2019.2.208>
- [3] Zhong, L., Wang, X., Cressault, Y., Teulet, P. and Rong, M. (2016) Influence of Metallic Vapours on Thermodynamic and Transport Properties of Two-Temperature Air Plasma. *American Institute of Physics*, **23**, Article ID: 093514. <https://doi.org/10.1063/1.4963245>
- [4] Cayet, S. and Dudeck, M. (1996) Equilibre chimique dans les mélanges gazeux en déséquilibre thermique. *Journal de Physique III*, **6**, 403-420. <https://doi.org/10.1051/jp3:1996130>
- [5] Schmitt, E., Commare, B., Panossian, A., Vors, J.-P., Pazenok, S. and Leroux, F.R. (2018) Synthesis of Mono- and Bis(fluoroalkyl)pyrimidines from FARs, Fluorinated Acetoacetates, and Malononitrile Provides Easy Access to Novel High-Value Pyrimidine Scaffolds. *Chemistry—A European Journal*, **24**, 1311-1316. <https://doi.org/10.1002/chem.201703982>
- [6] Koalaga, Z. (1991) Contribution à l'étude expérimentale et théorique des plasmas d'arcs électriques laminés. Thèse de doctorat, Université Clermont-Ferrand, Clermont-Ferrand.
- [7] André, P. (1995) Etude de la composition et des propriétés thermodynamiques des plasmas thermiques à l'équilibre et hors d'équilibre thermodynamique. Thèse de

- doctorat, Université Blaise Pascal, Clermont-Ferrand.
- [8] Bendjebbar, F., André, P., Benebakkar, M., Rochette, D., Flazi, S. and Vacher, D. (2012) Plasma Formed in Argon, Acid Nitric and Water Used in Industrial ICP Torches. *Plasma Sciences and Technology*, **14**, 683-692. <https://doi.org/10.1088/1009-0630/14/8/01>
- [9] André, P., Aubreton, J., Barinov, Y., Elchinger, M.F., Fauchais, P., Faure, G., Kaplan, V., Lefort, A., Rat, V. and Shkol'nik, S. (2002) Theoretical Study of Column of Discharge with Liquid Non-Metallic (Tap Water) Electrodes in Air at Atmospheric Pressure. *Journal of Physics D: Applied Physics*, **35**, 1846-1854. <https://doi.org/10.1088/0022-3727/35/15/305>
- [10] Pafadnam, I., Kohio, N., Yaguibou, W.C., Kagoné, A.K., Koalaga, Z. and André, P. (2023) Étude de la composition chimique des fluoroalkylamines utilisés en agriculture et en médecine dans le cadre de l'incinération par plasma entre 500 K et 20.000 K. *Journal International de Technologie, de l'Innovation, de la Physique, de l'Energie et de l'Environnement*, **8**, Article No. 1. <https://doi.org/10.52497/jitipee.v8i1.320>
- [11] André, P. and Koalaga, Z. (2010) Composition of a Thermal Plasma Formed from PTFE with Copper in Non-Oxidant Atmosphere. Part I: Definition of a Test Case with the SF<sub>6</sub>. *Material Processes*, **14**, 285-294. <https://doi.org/10.1615/HighTempMatProc.v14.i3.70>
- [12] Vacher, D. (2001) Détection, en temps réel, d'éléments métalliques présents dans les rejets atmosphériques industriels par torche à plasma à couplage inductif. Thèse de doctorat, Université Blaise Pascal, Clermont-Ferrand.
- [13] Kagoné, A, K. (2012) Caractérisation théorique de plasmas thermiques d'arc électrique de mélanges d'air et de vapeur d'eau: application au disjoncteur basse et moyenne tension. Thèse de doctorat, Université de Ouagadougou, Ouagadougou.
- [14] Kohio, N. (2016) Étude des propriétés thermodynamiques et des coefficients de transport des plasmas de mélanges d'air et de vapeur d'eau dans la gamme de température 500 K à 12000 K: Applications aux disjoncteurs basse et moyenne tensions. Thèse de doctorat, Université de Ouagadougou, Ouagadougou.
- [15] Hingana, H. (2010) Contribution à l'étude des propriétés des plasmas à deux températures: Application à l'argon et l'air. Thèse de doctorat, Université Toulouse III-Paul Sabatier, Toulouse.
- [16] Yaguibou, W, C. (2018) Influence des Aérosols sur les Performances des Disjoncteurs à Air Basse et Moyenne Tension. Thèse de doctorat, Université Joseph KIZERBO de Ouagadougou, Ouagadougou.
- [17] Cressault, Y. (2001) Propriétés des plasmas thermiques dans des mélanges Argon-Hydrogène-Cuivre. Thèse de doctorat, Université Toulouse III-Paul Sabatier, Toulouse.
- [18] André, P. (1997) The Influence of Graphite on the Composition and Thermodynamic Properties of Plasma Formed in Ablated Vapour of PMMA, PA6-6, PETP, POM and PE Used in Circuit-Breaker. *Journal of Physics D: Applied Physics*, **30**, 475-493. <https://doi.org/10.1088/0022-3727/30/3/022>
- [19] Hannachi, R. (2007) Etude expérimentale et propriétés radiatives d'un plasma thermique induit par impact laser à la surface de milieux aqueux H<sub>2</sub>O - CaCl<sub>2</sub>/MgCl<sub>2</sub>/NaCl. Thèse de doctorat, Université de Toulouse, Toulouse.
- [20] Kohio, N., Kagone, A, K., Yaguibou, W, C., Koalaga, Z. and Zougmoré, F. (2019) Water Vapor Influence on Thermodynamic Properties of Air-Water Vapor Mixtures Plasmas at Low Temperatures. *International Journal of Physics*, **7**, 66-72.
- [21] Kagone, A.K., Kohio, N., Yaguibou, W.C., Koalaga, Z. and Zougmoré, F. (2018)



Thermodynamic Properties Calculation of Air-Water Vapor Mixtures Thermal Plasmas. *Global Journal of Pure and Applied Sciences*, **24**, 37-49.

<https://doi.org/10.4314/gipas.v24i1.5>

- [22] Krenek, P. (2008) Thermophysical Properties of H<sub>2</sub>O-Ar Plasmas at Temperatures 400 - 50,000 K and Pressure 0.1 MPa. *Plasma Chemistry and Plasma Processing*, **28**, 107-122. <https://doi.org/10.1007/s11090-007-9113-z>
- [23] Koalaga, Z., Abbaoui, M. and Lefort, A. (1993) Thermodynamic Properties Calculation of C<sub>6</sub>H<sub>6</sub>O<sub>7</sub>N<sub>6</sub> Insulator Plasmas. *Journal of Physics D. Applied Physics*, **26**, 393-403. <https://doi.org/10.1088/0022-3727/26/3/008>